Engineering Journal of the University of Qatar, Vol. 15, 2002, pp. 223-240

DYNAMIC ANALYSIS OF A NOVEL MANPOWERED TRANSPORTATION VEHICLE WITH HIGH MECHANICAL EFFICIENCY

Tarek M. Abdel-Rahman and **Nabeel A. Al-Salem**
Mechanical Engineering Department
University of Qatar
P.O. Box 2713
Doha, Qatar
Email: tarek@qu.edu.qa & nabeel@qu.edu.qa

ABSTRACT

This paper evaluates the dynamics of a novel manpowered transportation vehicle. The vehicle has a novel mechanism that maximizes the mechanical input work and utilizes the weight of the rider for propulsion. The rider applies reciprocating stepping linear forces to drive chain and ratchet mechanism. The later transfer the reciprocating motion into a unidirectional rotational motion at the rear wheel to propel the vehicle. We analyzed the dynamics of the driving and transmission mechanism and derived the equations of motion, at first. Then, we evaluated the performance of the vehicle. Results show significant advantages of the novel driving mechanism.

KEY WORDS: Dynamic Analysis, Mechanical Mechanisms, Manpowered vehicle.

NOMENCLATURE

a	acceleration of the vehicle
A_e	effective body and vehicle area causing aerodynamic drag
B	normalized aerodynamic drag (defined by (9))
c_w	coefficient of wind aerodynamic drag
d	treadle stroke at man's foot
f_{ef}	equivalent rolling and mechanism friction coefficient
F	force
g	acceleration constant of gravity (= 9.81 m/sec^2)
G_r	driving to wheel gear ratio, $G_r = G_t \, . \, (r_w/r_d)$
G_t	transmission gear ratio

I_d non-dimensional inertia term defined by (6)
I_{mv} non-dimensional inertia term defined by (5)
I_s non-dimensional inertia term defined by (7)
k_{dw} radius of gyration of drive sprocket wheel
k_w radius of gyration of wheel
ℓ length
r_w radius of the wheel
r_d radius of the driving wheel
t time
t_f free fall time
t_p powering time
P Power
T_w torque transmitted to wheel
T_s steady state time period
v vehicle speed
v_d vehicle virtual speed in reflection to the drive speed
w_{dw} weight of the drive sprocket wheel in Newton
w_ℓ weight of man's leg in Newton (= 0.165 w_m)
w_m weight of man in Newton
w_s weight of a stepper in Newton
w_v weight of vehicle in Newton
w_{mv} weight to vehicle ratio ($w_{mv} = w_m/w_v$)
W work
W_f potential energy gained by ($w_m - w_\ell$) when it falling down a distance x_{pi}/G_r
α_m a factor when multiplied by w_m provides the driving force applied by the active leg
$\alpha_{m\ell}$ effective force factor (α_m) after subtracting legs raising effect (defined by (10))
ρ air density at sea level

1. INTRODUCTION

In the last few decades, many developments occurred in bikes and manpowered vehicles. Most of the developments were is the areas of tires, brakes, materials, suspensions, and gear transmission (Whitt and Wilson [1]). However, we still see the constant-length crank pedal dominating the market in spite of its inefficiency in transferring power. Each foot applies force during only 20% of the full pedal cycle. And, in addition the angle between the applied force and the tangent of the pedal path is greater than zero during most of the force application time. This results in

low input power even for high input pedaling forces. The later can be obtained by applying high hip and knee torques, which cause joint strains.

Many researchers have addressed the input power inefficiency of the drive system of bicycles, e.g. [2]-[6]. Miller and Ross [2] described a technique for generating a variable-ratio chain drives using non-circular driving sprocket to maintain constant angular velocity of the driven shaft for increasing the propulsion power. Han, Thomlinson and Tu [3] designed a non-circular front gear to maximize the output mechanical power. Freudenstein and Chen [4] introduced variable-ratio chain drives with non-circular front and rear sprockets. Su, Hsu and Tseng [5] obtained relationships between performance and indices of bicycle sprocket. Chen, Wang and Tseng [6] analyzed best arrangement of planetary gear train to maximize speed ratio range. In the aforementioned references the input and output motion were continuous.

Alternatively, reciprocating motion can be transferred into continuous rotational motion. Many patents, in the last few decades, considered transferring treadle motion into a continuous rotational motion at the driving wheel. A lot of them are impractical or dynamically inefficient. But, some seems to have promising potentials. Among those is the stepper bike of Lindsay and Wagner [7] shown in Fig.1. The rider applies a reciprocating vertical motion to power the bike and uses his body weight to augment his applied driving force. Treadle power [8] has recently introduced the stepper bike in the market. Millers and others [9] carried out electromyography analysis on stepper bikes. They showed that stepper bikes require less energy to drive and need smaller range of human limb movements to power the vehicle when compared to bicycles.

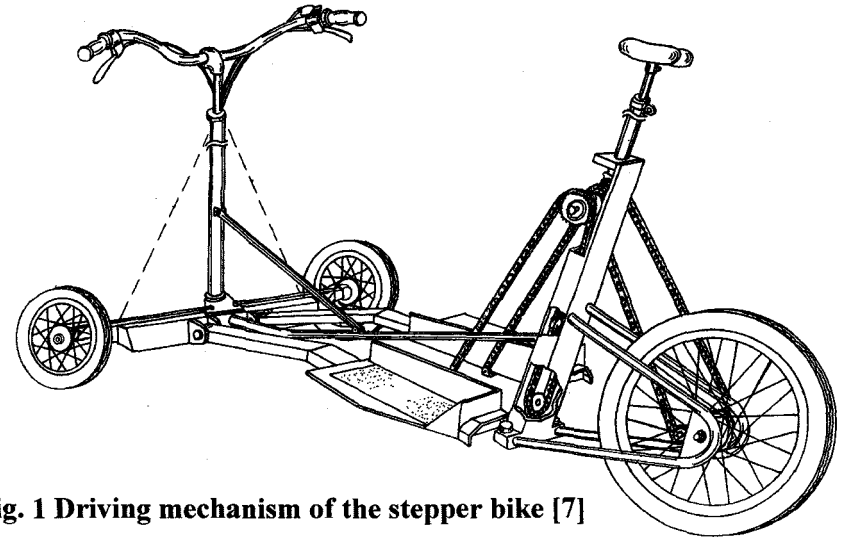

Fig. 1 Driving mechanism of the stepper bike [7]

Fig. 1 shows the driving mechanism of the stepper bike [7]. When the left treadle moves downward due to body weight, it rotates the upward sprocket counter clockwise to rotate a driving shaft through a ratchet mechanism. The shaft drives the rear wheel through a gear and chain mechanism. After the left treadle reaches its lowest position, the rider shifts his weight to the right treadle forcing it to move downward causing the rotation of the drive shaft in a clockwise direction. The gear and chain mechanism transfer the motion to the rear wheel. During the left and right leg strokes, the kinetic energy gained is used partially to accelerate the driving mechanism from zero velocity to proper value for ratchet engagement, at first, and to provide work for driving the bike. At the end of each stroke, some kinetic energy will still be available and will be lost during the collision of the treadle with the frame. To avoid loosing this energy, Abdel-Rahman and Fanni [10] used kinematics and power analysis approaches to obtain alternative driving mechanisms, which increase the propulsion power.

In this paper, we analyze the dynamics of the drive system of [7]. At first, we describe the kinematics in section 2. Then, in section 3, we derive the equations of motion, which can be used for seated and standing man positions, and, in section 4, we derive the power requirements. Section 5 shows performance evaluation results for selected parameters for a standing man position. Section 6 summarizes important findings and highlights interesting characteristics of the stepper bike.

2. DESCRIPTIVE KINEMATICS

Lindsay and Wagner [7] provide detailed description of the driving mechanism of the stepper bike. The mechanism is illustrated in a schematic diagram in fig. 2. The diagram depicts a tricycle with right and left lever-type pedals, 1 and 5 connected together by a single chain 2-3-4. Item 6 comprise two gears which drive one single shaft through two ratchets and a third gear rigidly connected to the shaft. The later transmits motion to a gear-ratchet mechanism, 7, fixed to the rear wheel. Items 1-6 and items 6-7 will be named the driving and transmission mechanisms respectively. The chain of part 3 is perpendicularly connected to the chain parts 2 and 4, and passes over a sprocket at its lower end, 8, which rotates in a direction normal to the page. Chains 2 and 4 drive the two gears connected to gear 6 via unidirectional ratchets. Pulling either chain 2 or 4 downward drives gear 6 in a clockwise direction. The motion is then transmitted to the wheel gear 7 to propel the rear wheels. For further details on how does the mechanism function the reader is advised to refer to Lindsay and Wagner [7]. Man applies a driving force on one foot to drive either stepper 1 or 5 until its maximum stroke is reached. And, then, he applies the force by the alternative foot. The driving leg is called the active leg and the other is called the passive leg. The foot applies the driving force along the

tangent of the path of its point of application. Hence minimum man force is needed for a required mechanical input power. Moreover, this force is fully or partially provided by the man's weight, hence reduces man's muscles strains.

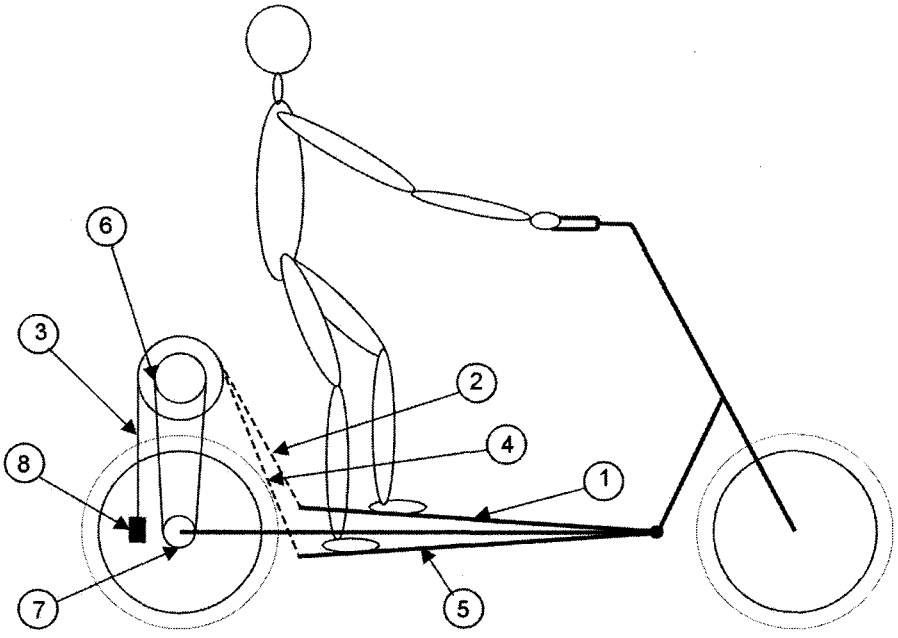

Fig. 2 Schematic diagram of the stepper bike

This driving mechanism arrangement is efficient from the dynamical point of view, but suffers from a kinematical drawback. The later is due to the reciprocating motion of the treadles. Each treadle begins its downward stroke from zero velocity. And due to the existence of ratchet mechanisms in the drive and transmission systems, there will be no input torque to the rear wheel until the treadle reaches certain velocity, at which the two parts of the ratchet mechanism have the same velocity.

Fig. 3 shows what happens to the speed of the driving mechanism as indicated by the dashed straight lines at the start of each leg stroke as compared to the vehicle speed indicated by solid lines. At start, t=0, the driving wheel, transmission, ratchets, and driving chains have zero speeds. Then, as soon as the driving chain starts to move the speed is transmitted to the drive and transmission ratchets immediately. The vehicle speed increases steadily until it reaches the maximum value v_{20} at the end of a one-leg stroke, d, after a powering period, t_{p1}.

The first stroke time is denoted by T_1. The periods t_{p1} and T_1 are equal at the first stroke. During the second stroke, by the alternative leg, a time t_{f2} will elapse until the transmission chain speed reaches the same speed of the wheel inner ratchet ring. The equivalent vehicle speed will be equal to v_{21}, and then a powering period will start and lapse for a period t_{p2}. The second stroke period T_2 becomes equal to $t_{f2} + t_{p2}$. This pattern continues on during speeding up resulting in the velocity pattern shown in Fig. 3. The speed at which the powering starts to occur is denoted by v_{21}, v_{31}, ..., v_{s1}. The last period represents the steady state case and it is characterized by the starting and ending velocity v_{s0}, inner velocity v_{s1} and period t_s. The wheels receives no driving forces during periods t_{f2}, t_{f3}, ..., t_{fs}, and receives driving forces; or is powered, during periods, t_{p1}, t_{p2}, ..., t_{ps}.

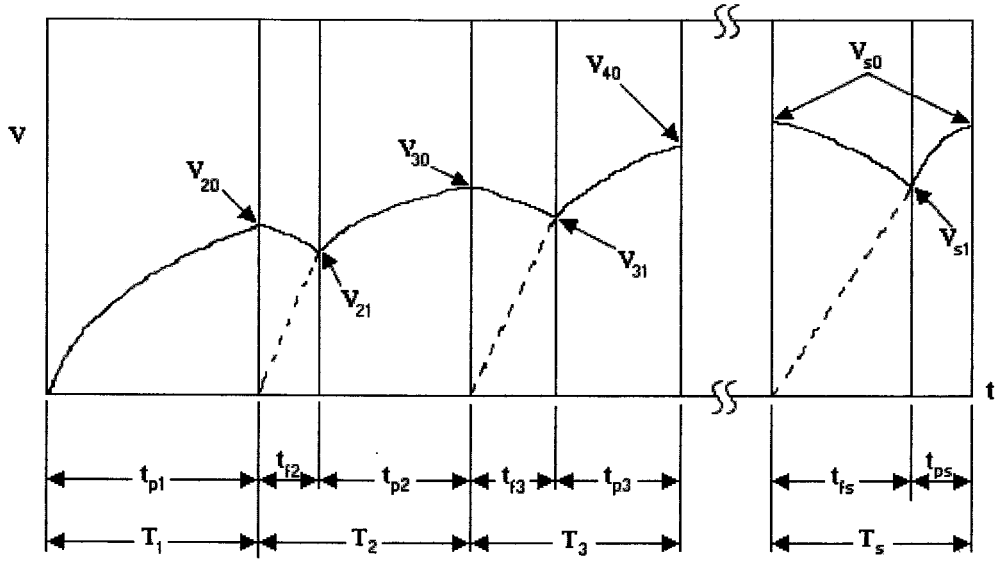

Fig.3 Speed increase versus time

3. DYNAMIC ANALYSIS

In this section, we derive the dynamical equations of motion for the driving and transmission mechanisms. Fig. 4 shows the free body diagrams of the steppers of the reciprocating drive. W_m and W_ℓ denote man's weight and man's leg weight. $\alpha_m W_m$ is the applied force by the active leg. α_m is a force factor. α_m equals 1 when man applies his weight, in a standing position, to

drive the vehicle. α_m is greater than 1 and could reach a value of 2.5, or 3 in extreme cases, if man applies additional pushing force (Hall [11]).

In Fig. 4, we assume that man is standing and applying force on the right foot, hence his right leg is active and his left foot passive, being left upward. F_r and F_ℓ are the forces in the driving chain on the right and left sides respectively.

F_{arx}, F_{ary}, $F_{a\ell x}$ and $F_{a\ell y}$ are the reaction components at the steppers pivots A_r and A_ℓ.

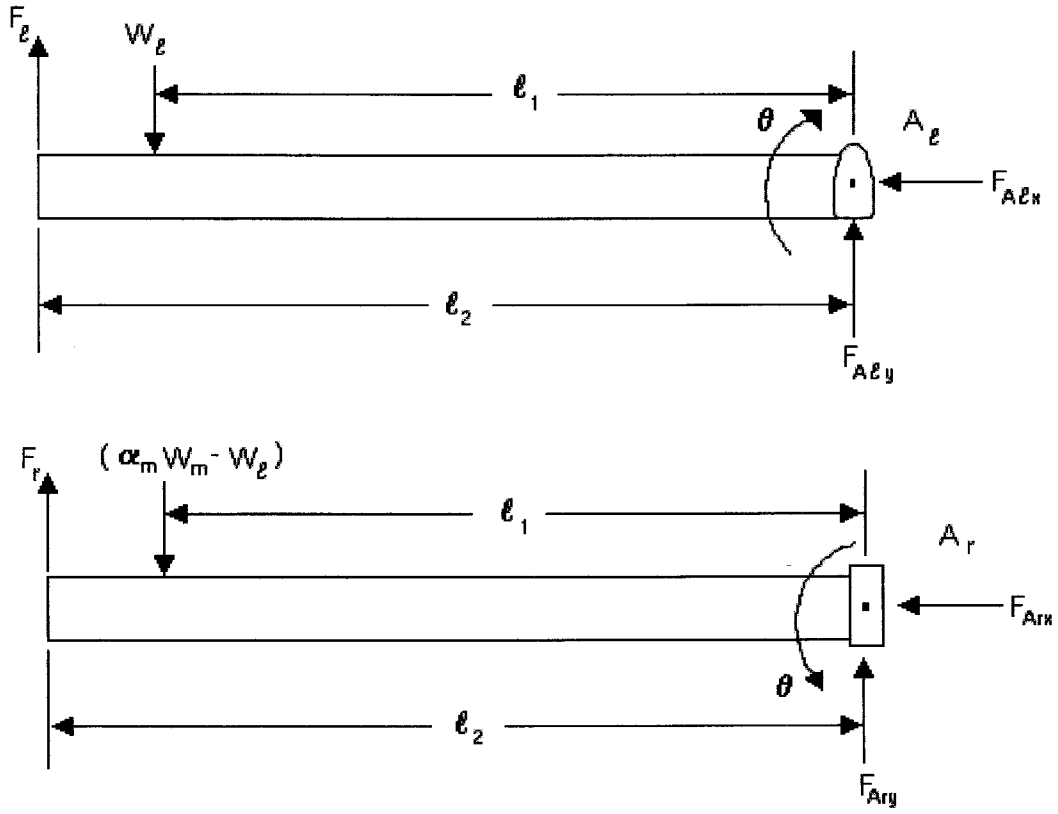

Fig.4 Free body diagrams of the left and right steppers while applying right leg force

Fig. 5 shows the free body diagrams of drive and transmission gears, and rear wheel. T_w represents the torque transmitted to the wheel and T_wG_t is its equivalent at the drive gear, where G_t is the transmission gear ratio, r_d and r_w are the radii of the drive gear and wheel respectively. R_w is the reaction at wheel contact with ground; and R_{adx}, R_{ady}, R_{awx}, R_{awy} are reactions at the center of rotation points A_d and A_w. To shorten derivation of equations of motion, we take moments of forces about points A_l, A_r, A_d and A_w. This cancels the effects of reaction forces at pivots and reduces unknowns.

In view of the illustration of Fig. 5 and after manipulation of the reduced equations of motion obtained from the moments equations we get:

$$[\, I_{mv}(w_{mv}) + I_d(\, G_r\,) \,.\, H(\, t\text{-}t_f\,) \,]\; a/g \;+ (B/w_{mv}) \,.\, v^2 \;+\; f_{ef} \,.\, (1+ 1/w_{mv}) \;= \\ (\alpha_{m\ell}/G_r\,) \,.\, (\ell_1 \,/\, \ell_2\,) \,.\, H(\, t\text{-}t_f\,)\,, \qquad (1)$$

to describe the motion of the vehicle and the following equation to describe the motion of the steppers:

$$v_d \;=\; G_r \,.\, (\ell_2 / \ell_1) \,.\, [\alpha_{ml} \;/\, I_s(w_{mv})\,] \,.\, g \;.\, t\,, \qquad (2)$$

where "v" and "a" are the speed and the acceleration of the vehicle defined by:

$$v = dx/dt, \qquad (3)$$

and

$$a = dv/dt. \qquad (4)$$

t is the time and x is the distant traveled by the bike; g is the gravity acceleration constant; and v_d is the speed of active drive system chain multiplied by G_r to yield virtual vehicle speed. The non-dimensional inertia terms are:

$$I_{mv}(w_{mv}) = 1 + (1/w_{mv}) \,.\, [\; 1+ 3. \,(w_w/w_v) \,.\, (k^2{}_w \,/\, r^2{}_w)\;] \qquad (5)$$

$$I_d(G_r) = (1/\, G^2{}_r\,) \,.\, [\; (\ell_1{}^2 / \ell_2{}^2\,) \;+\; (w_s/(2w_v)) \,.\, (\ell_1 \,/\, \ell_2\,) \;\;] \qquad (6)$$

$$I_s(w_{mv}) = 1 + (1/w_{mv}) \,.\, [\; (w_{dw}/w_v) \;+\; [(k^2{}_{dw}/r^2{}_d) \;+ (w_s/2w_v)] \,.\, (\ell_2{}^2 / \ell_1{}^2\,) \;] \qquad (7)$$

$$G_r \;=\; G_t \,.\, (r_w/r_d\,) \qquad (8)$$

$$B \;=\; \rho \,.\, c_w \,.\, A_e \;/\, (2w_v) \qquad (9)$$

$$\alpha_{m\ell} = \alpha_m - 2\,(w_\ell / w_m) \tag{10}$$

H is the Heaviside operator defined by:

$$H(t) = 0 \quad t < 0\ ,\ H(t) = 1 \quad t >= 0\ . \tag{11}$$

Solving equations (1-4) in distances and velocities within a powering period, T_i, yield:

$$x_{pi} = G_r\,.\,d - (1/2)\,.\,(\ell_1\,.\,I_s) / (\ell_2\,.G_r\,.\alpha_{ml}\,.\,g)\ v^2_{i,1}\,, \tag{12}$$

$$v^2_{i,1} = c_{1f} + (v^2_{i,0} - c_{1f})\,.\,e^{-c_{2f}(G_r d - x_{pi})}\,, \tag{13}$$

$$v^2_{i+1,0} = c_1 + (v^2_{i,1} - c_1)\,.\,e^{-c_2 x_{pi}}\,, \tag{14}$$

where x_{pi} is the distance traveled during ratchet engagement or power transmission period; $v_{i,0}$ is the speed at the start of the i^{th} stroke; and $v_{i,1}$ is the speed at the start of power transmission in the i^{th} stroke . The constants c_1, c_{1f}, c_2, and c_{2f} are given below:

$$c_{1f} = -\,w_{mv}\,.\,f_{ef}\,.\,(1 + 1/w_{mv})\ /\ B \tag{15}$$

$$c_1 = (w_{mv}/B)\,.\,(\alpha_{ml}/G_r)\,.\,(\ell_1/\ell_2) + c_{1f} \tag{16}$$

$$c_2 = 2\,.\,B\,.\,g\ /\ [\,w_{mv}\,(I_{mv} + I_d)\,] \tag{17}$$

$$c_{2f} = 2\,.\,B\,.\,g\,/\,[\,w_{mv}\,.\,I_{mv}\,] \tag{18}$$

As the driver continues applying forces during consecutive strokes, the speed $v_{i,0}$ increases, as illustrated in Fig. 3, until the steady state speed is reached when:

$$v_{i+1,0} = v_{i,0} = v_{s,0}\ . \tag{19}$$

In such a case, $v_{s,1}$ represent the initial velocity at the power transmission period of the steady state case. Using equation (19) and substituting, $v_{s,0}$ and $v_{s,1}$ in equations (13-15) yields three non-linear algebraic equations which can be solved to determine the variables x_{pi}, $v_{s,0}$, and $v_{s,1}$.

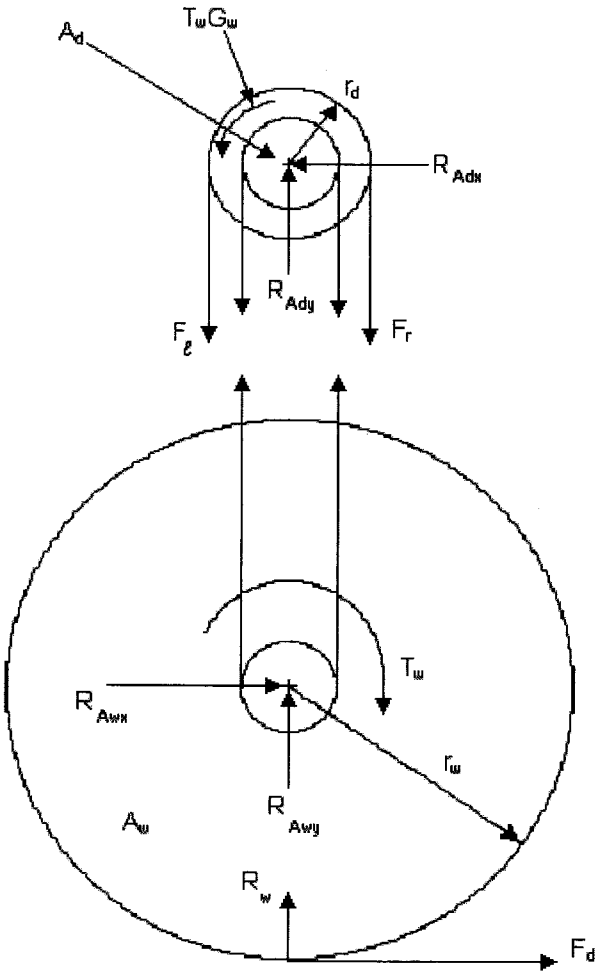

Fig.5 Free body diagram of the rear wheel, and drive and transmission gears

4. POWER REQUIREMENTS

During each stroke, man provides work for driving the vehicle to overcome inertia forces, aerodynamic drag, and rolling and friction forces. He, also, provides forces for raising his passive leg, and, in addition, does work to shift his weight from right foot to left foot and vice versa. The weight shifting work is taken at specific instanenous positions of thighs, shanks and trunks and hence is assumed to

be small in comparison to the work needed for driving the vehicle, as it occurs at a stand still position. In addition, we will assume that during the free fall, when the drive system is not propelling the vehicle, the energy gained from men's weight falling down provides sufficient work for raising the passive leg upward. Hence, no additional man muscle – based power will be needed to raise the passive leg. From the above description of work needed to drive the vehicle, we can state that

$$W = W_{idfr} - W_f \ , \tag{20}$$

Where W is the net work done by man, W_{idfr} is the work needed to overcome inertia, aerodynamic drag, friction and rolling resistance forces; and W_f is the potential energy gained from man's partial weight, $w_m - w_\ell$, falling through a distance x_{pi}/G_r . The distance traveled by the weight during power transmission. At steady-state, dividing equation (20) by T_s yields the average power

$$P = P_{idfr} - W_f / T_s \ . \tag{21}$$

P_{idfr} is the power needed to overcome the dynamical resistance of motion and the last term in equation (21) represents the power saving gained at steady state, via potential energy of falling weight, by using the stepper bike. If the transient motion is considered further, energy savings is expected in comparison to regular bikes.

5. PERFORMANCE EVALUATION

To evaluate the dynamics characteristics of the considered bike, we will use the following constants:

$\rho = 1.226\ kg/m^2$, $A_e = 0.7m^2$, $c_w = 0.5$, $f_{ef} = 0.004$, $\ell_1 \approx \ell_2$, $w_v/g = 25\ kg$,

$g = 9.81 m/sec^2$, d=0. 3 m, $k_w \approx r_w$, $k_{dw} \approx r_d$, $w_{dw}/w_v \approx 0$, $w_s/w_v \approx 0$,

in all computations in this section. To compute the starting acceleration, we substitute v = 0 in equation (1). Fig. (6) shows the starting, or maximum, acceleration at various gear ratios, G_r, under different w_{mv} weight ratios 1, 2 and 4. The Figure depicts that the starting accelerations of heavier riders is larger than lighter ones. This is attributed to the higher propelling forces provided by heavier weights. In addition, the same Figure shows that there is a maximum that occurs for each w_{mv} ratio. Maximum accelerations occur

in the region $0.8<G_r<2$. The later two findings differ from regular bike performance. As heavier riders start with smaller accelerations and the smaller the gear ratio the larger starting acceleration the rider gets.

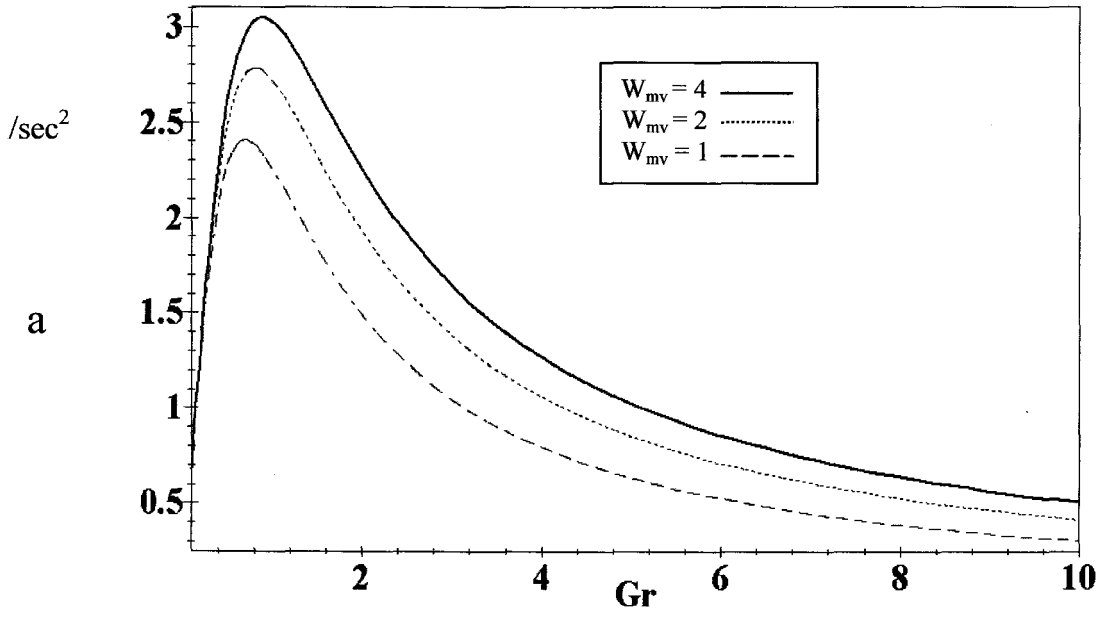

Fig. 6 Variation of the maximum acceleration versus the gear ratio for (α=1)

Solving equations (12-14, and 19) for the steady-state velocity yields the results shown in Figs. 7-9. Fig. 7 shows variation of the maximum steady-state velocity at various gear ratios, G_r, for various operating force levels, α. As expected, higher speeds can be obtained by increasing α, the applied force factor. Also, it is of interest to note that the maximum speed reaches a value of 14 m/sec that is equivalent to 50.4 km/hr when, continuously, applying a force equal to 1.2 times the weight at each leg stroke. Fig. 8 shows the maximum steady-state velocity for a normal application of leg force equal to man's weight and accordingly requires low muscle forces for comfortable operation. The Figure depicts that heavier men can achieve higher speeds at some gear ratio, G_r, and shows that the maximum speed increases as G_r increases until a supreme value is reached and then decreases with further increase of G_r. The supreme speed that can be achieved by a man that weighs four times the weight of the vehicle is about 12.5 m/sec, which is equivalent to 45 km/hr. No further increase of speed is possible via increasing the gear ratio G_r. This was expected, as further increase in G_r reduces the propelling

force. The increase of speed due to increase of G_r at smaller gear ratio range is attributed to the increase in the powering duration which the force is transmitted to

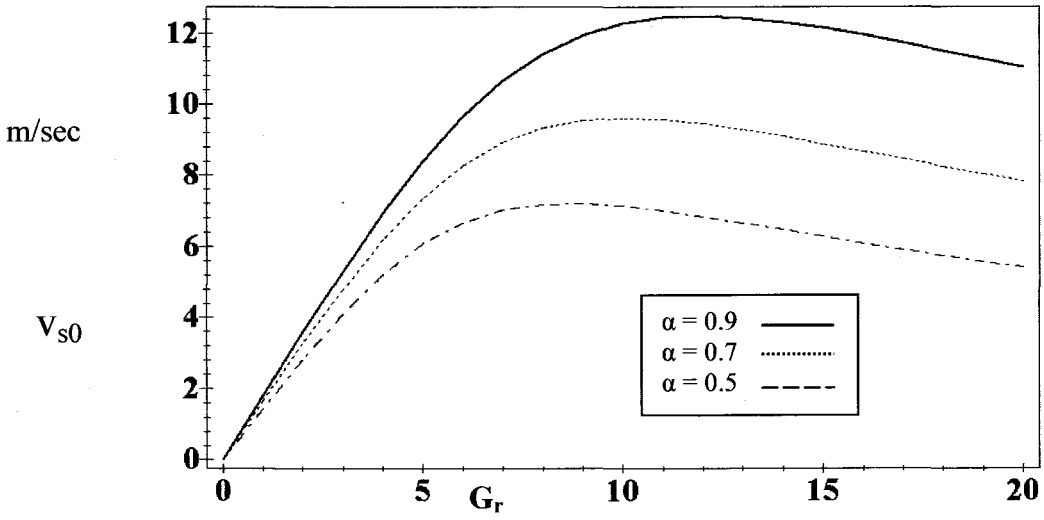

Fig. 7 Variation of maximum speed versus the gear ratio (for $w_{mv} = 4$)

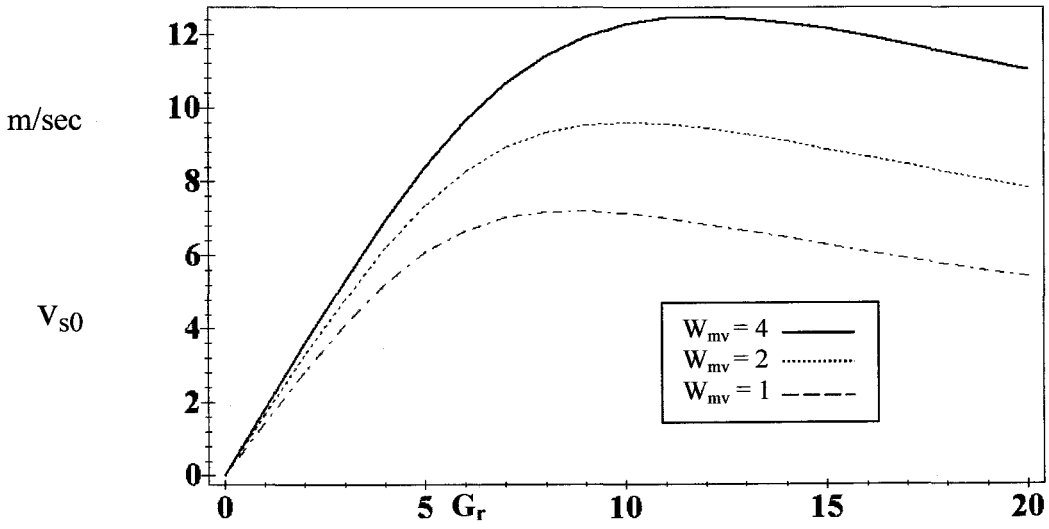

Fig. 8 Variation if the maximum steady-state speed versus the gear ratio (for α = 1)

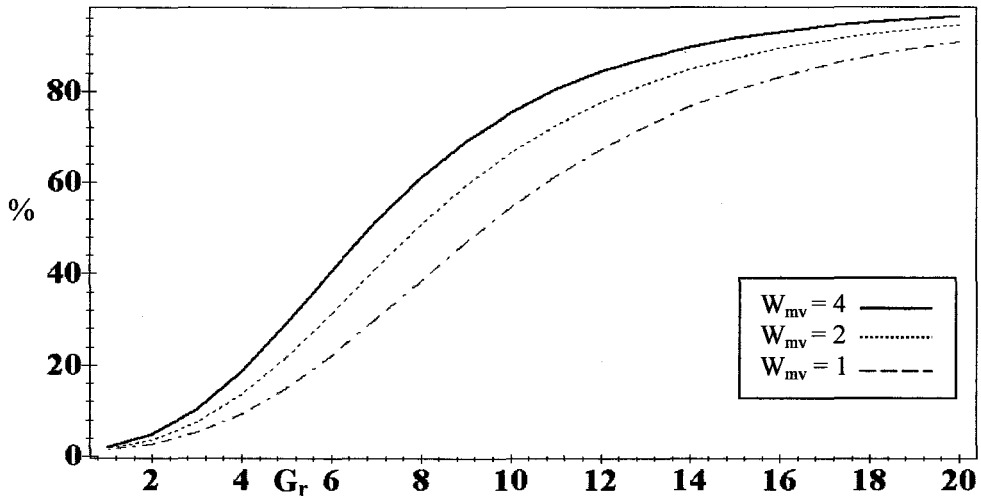

Fig. 9 Variation of the powering distance percentage versus the gear ratio (for $\alpha = 1$)

the wheel to propel the vehicle. Fig. (9) clarifies this point. The Figure shows the percentage of the stroke, d, which is utilized in powering the vehicle at the steady-state speeds.

To evaluate power requirements, we used equation (20) and the parameters specified at the beginning of this section to get the results shown in Figs 10-12. Fig. 10 shows the power requirements to drive the vehicle by a man whose weight ratio is $w_{mv} = 4$ at the steady-state speeds obtained at various G_r for powering force factors: α=.8, 1, and 1.2. In addition to the later value of w_{mv}, two other values w_{mv} =1 and w_{mv} =2 were considered. For these values, Fig 11depicts power requirements for α=1 at steady-state speeds attainable at various gear ratios. Figs 7-11 show that power requirements increase in proportion to v^2_{s0}. To compare power needed for driving a stepper bike with that needed for regular bike at the same speed, we computed requirements at α=1 and w_{mv} = 4. Fig 12 shows a comparison of power requirements at various gear ratios. The Figure depicts that the stepper bike requires 40-60% of the power needed for driving bikes at similar speeds, a significant reduction, of course. Thus, higher speeds can be achieved with lower manpower.

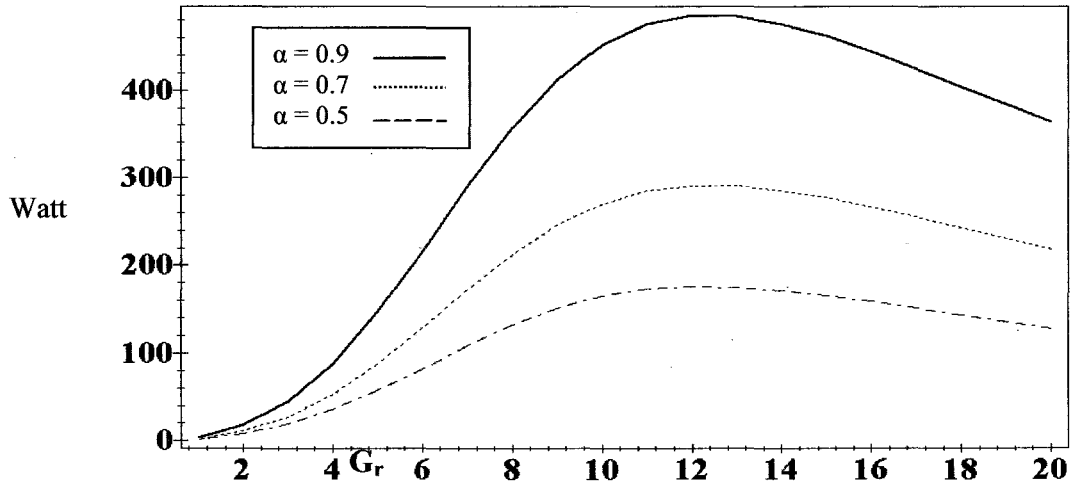

Fig. 10 Power requirement at various forcing conditions (for $w_{mv} = 4$)

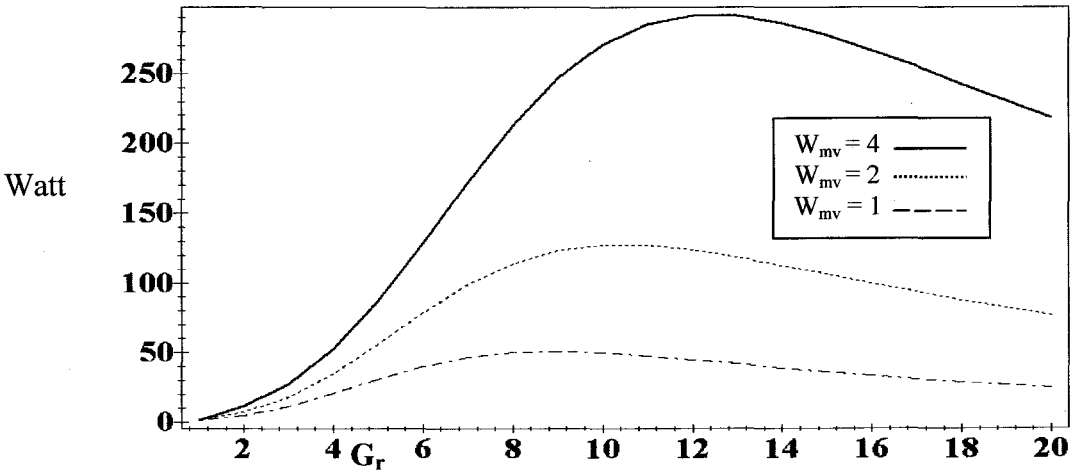

Fig. 11 Power requirement at various, w_{mv}, weight ratios (for α=1)

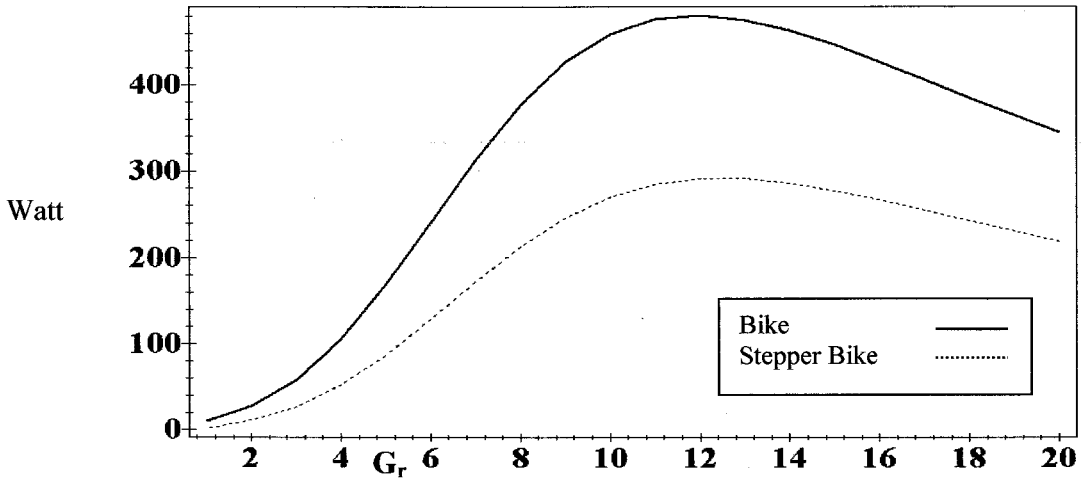

Fig.12 Comparison of power requirements versus power required for driving bikes with same maximum speeds attainable at G_r (for w_{mv}=4 and α=1)

6. CONCLUSION

In this paper, we have considered a novel manpowered vehicle, the stepper bike, which transfers a reciprocating linear motion into a continuous rotational one. We derived the equations of motion and analyzed its performance at a range of practical parameters. Results showed outstanding characteristics in speed and power requirements. Riders with a weight to vehicle ratio of 4 can achieve 45 km/hr speeds by using properly selected gear ratios. Moreover, it was observed that higher speeds could be achieved as the weight ratio increases. This finding favors heavy weight riders who shy away from regular bikes because of its performance deterioration due to their additional weight. On the power requirements side, the stepper bike requires 40-70% of the power needed to drive regular bikes at the same speed. This is attributed to the utilization of potential power gained from the rider falling weight during the propelling action. The speed and power advantages imply that the stepper bike outperforms the regular bike.

REFERENCES

1. **Whitt, F.R.** and **Wilson, D.G., 1982** ,Bicycling Science, The MIT Press.

2. **Miller, N.R., Ross, D., 1980,** "The Design of Variable-Ratio Chain Drives for Bicycles and Ergometers – Application to a Maximum Power Bicycle Drive," ASME, Journal of Mechanical Design, Vol. 102 pp: 711-717.

3. **Han, R.P.S., Thomlinson, M.A., Tu, Y.S., 1991** "Kinematics and Kinetics of a Non-Circular Bicycle Drive System," Mech. Mach. Theory, Vol. 26, No. 4, pp: 375-388.

4. **Freudenstein, F., Chen, C.-K., 1991,** "Variable-Ratio Chain Drives with Noncircular Sprockets and Minimum Slack-Theory and Application," ASME, Journal of Mechanical Design, Vol. 113 , pp: 253-262.

5. **Su, S.-H., Hsu, P.-H., Tseng, C.-H., 1997,** "Analysis of Tooth Profiles on Bicycle Sprockets," Journal of the Chinese Society of Mechanical Engineers, Vol. 18, No. 4 , pp: 331-339.

6. **Chen, J.-L., Wang, C.-C., Tseng, C.-H., 1998**, "On the Discrete Optimization of Multi-Speed Hubs in Bicycles," Journal of the Chinese Society of Mechanical Engineers, Vol. 19, No. 5, pp: 497-507.

7. **Lindsay, S.M.W., Wagner, J.H., 1995**, "Treadle Drive System with Positive Engagement Clutch," U.S. Patent No. 5451070, http://patft.uspto.gov/netahtml/srchnum.htm

8. Treadle Power, Inc., http://www.stepngo.co, 800-648-7335 USA & Canada.

9. **Miller, M.S., Martin, J.A., Peach, J.P., Lindsay, S., Keller, T.S., 1999**, "Electromyographic Analysis of a Human Powered Stepper Bike," Proceedings of the 1999 IEEE/EMBS 25th Annual Northeast Bioengineering Conference , pp: 120-121.

10. **Abdel-Rahman, T.M.** and **Fanni, M., 2001,** "New Driving Mechanism for Man-Powered Vehicles," 7th International Conference on Production Engineering, Design and Control, 13-15 Feb., Alexandria, Egypt, pp. 809-821,

11. **Hall, S. J., 1999 ,** Basic Biomechanics, MacGraw-Hill, 3rd Ed., pp. 398-399,.